13

Time-of-flight linear mass reflectron with various interfaces

© N.N. Aruev, P.A. Romanov, R.V. Tyukaltsev, I.L. Fedichkin

Ioffe Institute,
194021 St. Petersburg, Russia
e-mail: aruev.mass@mail.ioffe.ru , romanovpa227@gmail.com

Received August 23, 2023
Revised September 26, 2023
Accepted October 23, 2023

Magnetic-free time-of-flight mass spectrometers (TOF) are widely used in various fields of science and industry due to their simplicity, reliability, low cost and unique analytical characteristics, such as: high analysis speed, unlimited mass range, the ability to obtain an overview spectrum in one measurement cycle, sufficiently high resolution and sensitivity and the ability to work in a synchronous mode of spectrum detection, selecting different parts of the mass peaks. Time-of-flight instruments without a reflector, mass spectrometers with a V-shaped ion trajectory, and linear mass reflectrons are considered. All these devices are united by the fact that they used an ion source of the Nier type with ionization of volatile gas molecules by electron impact. On the one hand, this greatly limits the scope of application of VPMS, since it excludes their use in biology, pharmaceuticals, proteomics, etc., and on the other hand, it allows the use of different interfaces for introducing various natural and technogenic samples into the mass liquid and gaseous states and develop new research methods.

Keywords: mass reflectron, interface for sample injection, mass spectrum.

DOI: 10.61011/JTF.2024.01.56915.205-23

Introduction

The authors of the first time-of-flight non-magnetic mass spectrometer [1] named their device velositron, which probably means an ion velocity meter. Its idea is extremely simple. The ions will fly in field-free space at different speeds if an ion source is placed at one end of a pipe with a high vacuum and all the ions formed in it are given, for example, a positive impulse: the velocities of light ions will be higher than the velocities of heavy ions. And ion detector will register light ions first, and then increasingly heavier ions if it is placed at the other end of the pipe. This is how the ions are separated based on the velocity or based on the time of flight. The time of flight T of ions with mass M and charge e of the distance from the source to the detector L is determined by the expression

$$T = L\sqrt{\frac{M}{2eU_0}}, \tag{1}$$

where U_0 — the potential difference accelerating ions. Then the resolution of the mass spectrometer based on the mass peak is determined by

$$R = \frac{M}{\Delta M} = \frac{T}{2\Delta t}, \tag{2}$$

where T — the time of flight of the mass ions M from the source to the detector, and Δt — the duration of the ion packet with one mass-to-charge ratio M/q on the input plane of the detector or the spread of the arrival time of ions of one mass per detector.

An aberration model describing the broadening of the mass peak is usually used for designing time-of-flight mass spectrometers (TOFMS) with grids

$$\Delta t = \sum \Delta t_i + \sqrt{\sum (\Delta t_k)^2}, \tag{3}$$

where Δt_i — the average value of the time of passage of a single ion from the source to the detector and Δt_k —the spread of the time of arrival of ions at the detector caused by various aberration factors. The following aberrations are typical for any TOFMS with grids:

1) Δt_{tat} — broadening of the ion packet associated with the unavoidability of the ion reversal time (turn around time) during the action of a positive rectangular pulse (usually called an ejection pulse), which is applied to the first electrode limiting the ion source ionization zone. This aberration is associated with the transfer of kinetic energy from an electron to a molecule at the moment of an electron impact, as well as with the initial thermal velocities of molecules, which can be directed in the direction opposite to the direction of the electric field lines;

2) Δt_v — broadening of the ion packet caused by the scattering of ions at initial velocities during the ionization process, associated with the distribution of molecules in space inside the ionization zone bounded by two grid electrodes;

3) $\Delta t_{\Delta x}$ — broadening of the ion packet associated with the finite size of the ionization region in the direction of ion ejection;

4) Δt_d — broadening of the ion packet due to the finite response time of the detecting device to the arrival of one ion;

5) Δt_{MCP} — broadening of the ion packet caused by the depth of the entrance of the microchannel plate of the detector;

6) Δt_{grid} — broadening of the ion packet because of ion scattering on the microheterogeneities of the grid fields. Aberrations 1–3 usually have the largest magnitude.

A number of important conclusions can be drawn using the principle of operation of TOFMS and formulas (1) and (2). The mass range of the device is unlimited since ions of different masses from the lightest to the heaviest are ejected from the source simultaneously and it is determined only by the capabilities of the detection system. This is a fast-acting device since the entire mass spectrum is recorded as ions of different masses arrive at the detector after one ejection pulse. The resolution of the device is directly proportional to the time of flight or the length of the ion flight path, i.e. practically the length of the vacuum chamber. The resolution of time-of-flight devices depends on the mass of the measured ions, i.e the resolution is low in case of light masses, and the resolution is high in case of on heavy ions which makes it possible to study huge biological molecules. We believe that the dependence of the resolution on the amplitude of the ejection pulse is ambiguous, since the trajectory length and ion velocities depend on the scattering of ion packets on grids, on atoms and molecules of residual gases, on the impact of surface charges on the walls of the vacuum chamber, etc.

The first Soviet TOFMS [2] was known for the fact that its vacuum chamber and all internal devices were made of glass and practically contained no metals, except for electric molybdenum inlets, a tungsten cathode and grids, to which the necessary potentials were supplied. It was noted in later papers [3,4] and experimentally confirmed that the TOFMS can operate in such a mode when only certain ion packets are admitted to the detector, i.e. ions are registered selectively. Subsequently, this mode was called the synchronous detection mode. The main disadvantage of TOFMS is the low resolution.

1. Mass reflectron

The idea of usage of an ion reflector in TOFMS to increase its resolution was first published in the paper [5], but it was not implemented in practice and is practically unknown. B.A. Mamyrin registered the copyright certificate about 10 years after that [6], which also went unnoticed at first. The publication of the new principle of focusing of ion packets in the TOFMS [7] also did not arouse much interest in the research community. And only an article about a new really functioning high-resolution non-magnetic TOFMS, called the mass-reflectron by the authors [8], aroused a broad interest among both scientists and instrument manufacturers.

Many companies around the world began to produce mass reflectors, which began to be widely used in various scientific studies, in various industries to study kinetics and control rapidly occurring processes. A great many articles, reviews, and monographs cover the operation of such devices, and we will not even try to list the reasons and purposes of the usage of mass reflectors, but simply state that they have all the above-mentioned features and advantages of TOFMS and plus a significantly higher resolution. Here, obviously, it should be said that the first mass reflectors had a V-shaped trajectory of ion movement, and this immediately determined some parameters and features of the devices.

Firstly, the use of a reflector in the TOFMS practically doubles the resolution of the device by increasing the trajectory and time of flight of ions with the same dimensions of the vacuum chamber. It is assumed that the reflector consists of three parallel electrodes that form two flat gaps. Moreover, the first two electrodes are grids, and the third electrode can be either a grid or a solid metal plate under a potential exceeding the amplitude of the ejection pulse in the ion source. The ions are slowed down in the first decelerating gap and the ion velocity drops to zero in the second reflecting gap, the direction of movement of ions change, they accelerate in both gaps, enter the field-free drift space, where the packets are further separated based on the time of flight and the ions reach the detector. Secondly, it turned out that the time of flight of ions with a single value M/q is compensated in the reflector, i.e. in a package consisting of one ion variety. Ions that received more energy in the source will pass through the reflecting gap to a greater depth than ions with average energy, the ions slow down to zero speed, change their direction of movement to the opposite direction, exit the reflector and spend more time on this, and ions with lower energy will spend less time passing through two gaps of the reflector than ions with the medium energy. This is how the ion time of flights are compensated. The relative change of the time of flight is of the order of 10^{-4} with initial ion energy spreads of several percent of the average energy according to [8]. This means that the duration of the ion packets Δt, with a single value M/q, becomes small and the resolution increases. The reasons for the increase of the duration of ion packets (temporary aberrations), presented above (6 points), are described in more detail in [9,10] and here we will not discuss them in detail, since this is not the topic of this paper. However, let's say that the compensation of the ion energy spread occurring in the two gaps of the reflector concerns only the aberration Δt_v — i.e., the broadening of the ion packet caused by the scattering of ions along the initial velocities during the ionization process. The other 5 aberrations are not affected by the reflector.

Recall that the length of the vacuum chamber of the mass reflectron [8] was 1000 mm, and the pipe diameter was 160 mm. Let us also pay attention to the fact that the large diameter of the vacuum chamber of the mass-reflectron with a V-shaped trajectory of ion movement made it possible to place a electron beam magnetic focusing system inside the device consisting of two ferrite pole tips with a diameter of 30 mm and a thickness of 10 mm, as well as an iron yoke with a cross section of 1,see [2], which produced a magnetic field of the order of 200 Oe [11]. An ion source with magnetic focusing of the electron beam expands the

capabilities of the mass-reflectron, since, firstly, it increases the resolution and sensitivity of the device, and, secondly, it allows operation at low energies of ionizing electrons close to the ionization potentials of the studied substances. As a result, the TOFMS [8] with an ion source in which the electron beam is magnetically focused has a resolution at half-height of mass peaks in the mass range of 500 amu of the order of 4000–5000. Another element that was introduced into the mass analyzer was an electric heater located in close proximity to the ion source. A quartz crucible with an internal volume of approximately 5 mm^3 is placed in the heater, in which the test sample is located. The crucible with the sample could be heated to 900°C, while the temperature was controlled by a thermocouple.

The formation of metallofullerenes was studied [12], the fullerenes enriched with D-isotope ^{13}C were analyzed [13] and trace amounts of gold were detected in natural samples and chemical compounds [14] owing to high analytical characteristics of the mass reflectron, which includes an ion source with electron beam magnetic focusing and an internal heating element for the separation of volatile fractions from the studied samples.

Despite the successes achieved, further developments showed that the mass reflectron with a V-shaped trajectory of ion movement has some disadvantages: the difficulty of focusing the ion beam at the angles of ion departure from the source, the large size of the mass analyzer and the entire device as a whole, and in addition, a number of tasks appeared that required a small, portable instrument.

2. Linear mass reflectron

As a result of the study, a new scheme of the ion-optical mass-reflectron system was proposed, the so-called linear mass-reflectron [15]. The ions move along trajectories in linear mass-reflectron that are parallel to the axis of the mass analyzer chamber. The ion source is located almost in the middle of the mass analyzer. The ions formed in the ionization zone of the source are ejected from it by a rectangular pulse, accelerated in the first accelerating gap, fall into the field-free drift space and further into the two-gap reflector. The ions accelerate again after changing of the direction of movement in the reflecting gap of the reflector, they fly in the opposite direction through the ion source, the second drift space and enter the detector, which comprises a microchannel plate (MCP) or an assembly of two MCP, where the signal is amplified. The resolution of a linear mass spectrometer (Fig. 2) like the resolution of a simple TOFMS (Fig. 1, *a*) and a mass-reflectron with a V-shaped trajectory of ion movement (Fig. 1, *b*) is determined by the formula (2) and all the advantages and benefits inherent in TOFMS are preserved.

The high analytical performance of linear TOFMS, their speed, unlimited mass range, as well as the rather small dimensions and weight of the devices have made them indispensable in the study of fast-flowing chemical, physical,

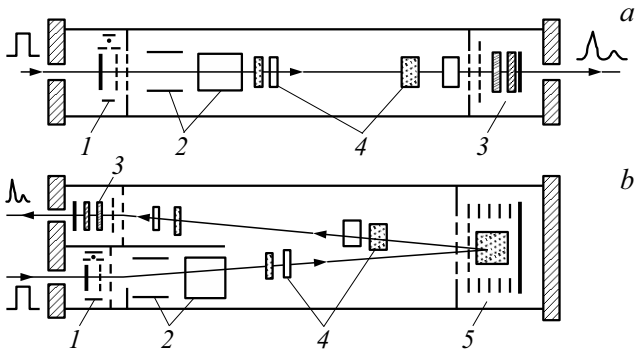

Figure 1. TOFMS of a conventional circuit (*a*) and a mass-reflectron circuit (*b*): *1* —ion source, *2* — deflecting plates, *3* — ion detector, *4* — ion packages, *5* — ion reflector.

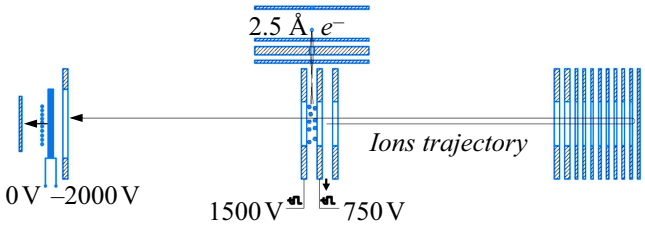

Figure 2. The diagram of linear TOFMS.

metallurgical, biological and other processes taking place in nature, industry, and science.

We will start with the interface designed for the admission of gas samples since mass spectrometers were originally designed and used for the study of volatile substances. A piezoelectric leak is mounted on the removable flange from the outside, into which the test sample is injected, and a metal capillary is fixed inside the mass analyzer chamber from the flange, going to the ionization area of the source, so that the injected gas sample enters the source without loss and is analyzed by the instrument. Stainless steel is used as the material for the leak and capillary, which is quite passive with conventional gases. One of the first applications of the linear mass reflectron was its use for continuous monitoring and control of converter processes in ferrous and non-ferrous metallurgy based on mass spectrometric analysis of gases leaving the converter and finding a connection between the composition of the exhaust gases and the carbon content in the iron melt, i.e. determining the grade of steel being smelted [16].

The following paper studied the process of electron beam full oxidation of sulfur dioxide, obtained, for example, by smelting copper in the presence of ammonia and water vapor into ammonium sulfate, which is a valuable nitrogen fertilizer [17]. The small dimensions and weight, as well as the sufficiently high resolution and sensitivity of the linear mass-reflectron, allow it to be used directly on large physical installations for studies, for example, in the cyclotrone of the Ioffe Physical-Technical Institute in various parts of its vacuum system, to determine the contribution of various

components to the residual vacuum and to develop methods to modernize the cyclotron vacuum system [18].

Here, it is probably necessary to recall another unique property of the TOFMS, which was mentioned earlier, that only these devices allow for operation in synchronous mode for detection of individual mass peaks [3]. This makes it possible to reliably analyze the chemical and isotopic compositions of gas mixtures, for example, a hydrogen-helium mixture containing radioactive tritium. This study was performed jcite19 and it was shown that the presence of tritium in the gas sample does not affect the measurement accuracy of other components of the gas mixture. In our opinion, only these devices can ensure reliable analysis of fuel gas mixtures for thermonuclear reactors.

3. Interfaces for entering samples

Fig. 2 shows that the ion-optical scheme and the design of the linear mass-reflectron are such that they do not allow the use of magnetic focusing of an electron beam ionizing atoms and molecules of the studied substance, since there is practically no free space for placement of magnetic poles inside the analyzer chamber. Therefore, we used the other method and began to develop various interfaces for introduction of various samples into the device for expanding the scope of application of the linear TOFMS and expanding its capabilities. We installed a miniature heating element inside the device for examining solid samples like in study [12,13] (Fig. 3). A quartz tube is placed inside this heater is placed. It is a crucible with an inner diameter ≤ 2 mm and height $\sim 10-12$ mm which accommodates a solid sample. The upper open end of the crucible is located near the ionization zone of the ion source. The crucible is heated, its temperature is measured using a thermocouple and the mass spectrum of gases and volatile components released from the sample is recorded at every 100°C, i.e. chemical and isotopic analysis of substances is performed.

The first substance studied using this interface was nanodiamonds obtained by detonation. The study of the properties of nanodiamond surface showed that these properties strongly depend on the processing methods and the

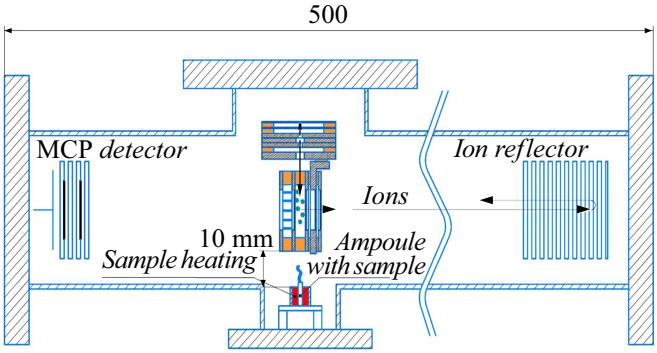

Figure 3. The diagram of a linear TOFMS with an installed sample heating system.

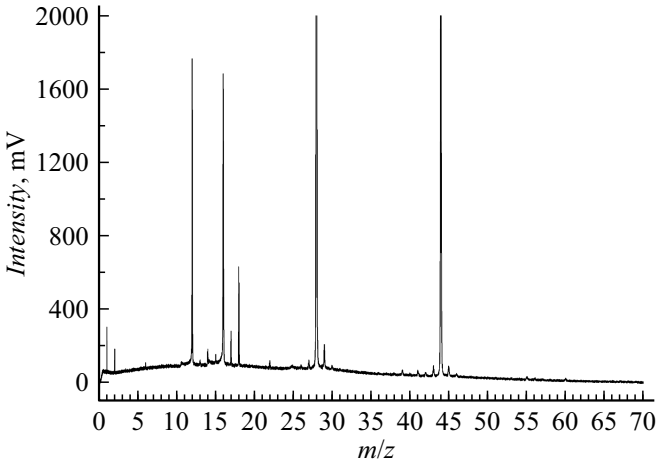

Figure 4. Formation of a „hump“ on the mass spectrum obtained by heating of nanodiamond sample to a temperature of 800°C.

composition of gas impurities in nanodiamonds. The found patterns made it possible to improve the quality and yield of nanodiamonds with various processing methods of the resulting product [19]. Samples of detonation nanodiamonds were heated from room temperature to 900°C in increments of 100°C during the analysis and it was noticed for the first time that the baseline of the mass spectrum in the low-mass region is curved and a hump forms on it at temperatures above 700°C. The mass spectrum shown in Fig. 4 contains peaks $^1H^+$ H_2^+ ($m/z = 1$ and 2) amu, peak $^{12}C^+$ (12 amu), peak, with mass 16 amu, probably CH_4^+ and peaks with masses of 28 and 44 amu — carbon monoxide and dioxide. The water H_2O and the hydroxyl group OH^+ (ion masses 17 and 18 amu) peaks are quite small at such high heating temperatures. The largest peaks in the mass spectrum of heated nanodiamonds contain carbon.

Perhaps this curvature of the baseline of the mass spectrum is attributable to the thermoelectron emission from the heater tungsten wire and the ionization of atoms and molecules outside the ionization zone in the source, but, in our opinion, this effect requires further careful study and explanation.

This is the reason why we did not heat the crucible above 700°C in our next study with the interface for solid samples when we analyzed the composition of the absorbed gases with a protective graphite layer that covers the entire inner surface of the Globus-M2 Tokamak vacuum chamber facing plasma [20,21]. Graphite powder removed from the surface of the protective tiles with a sharp scalpel was used as samples. This powder was placed in a quartz crucible, heated from room temperature to 700°C in increments of 100°C and the mass spectra of the released gases were recorded. Desorption curves of most of the gas components were constructed on the basis of the obtained spectra. The analysis and study of desorption curves allowed for determining where and how deep these sorbed gases are

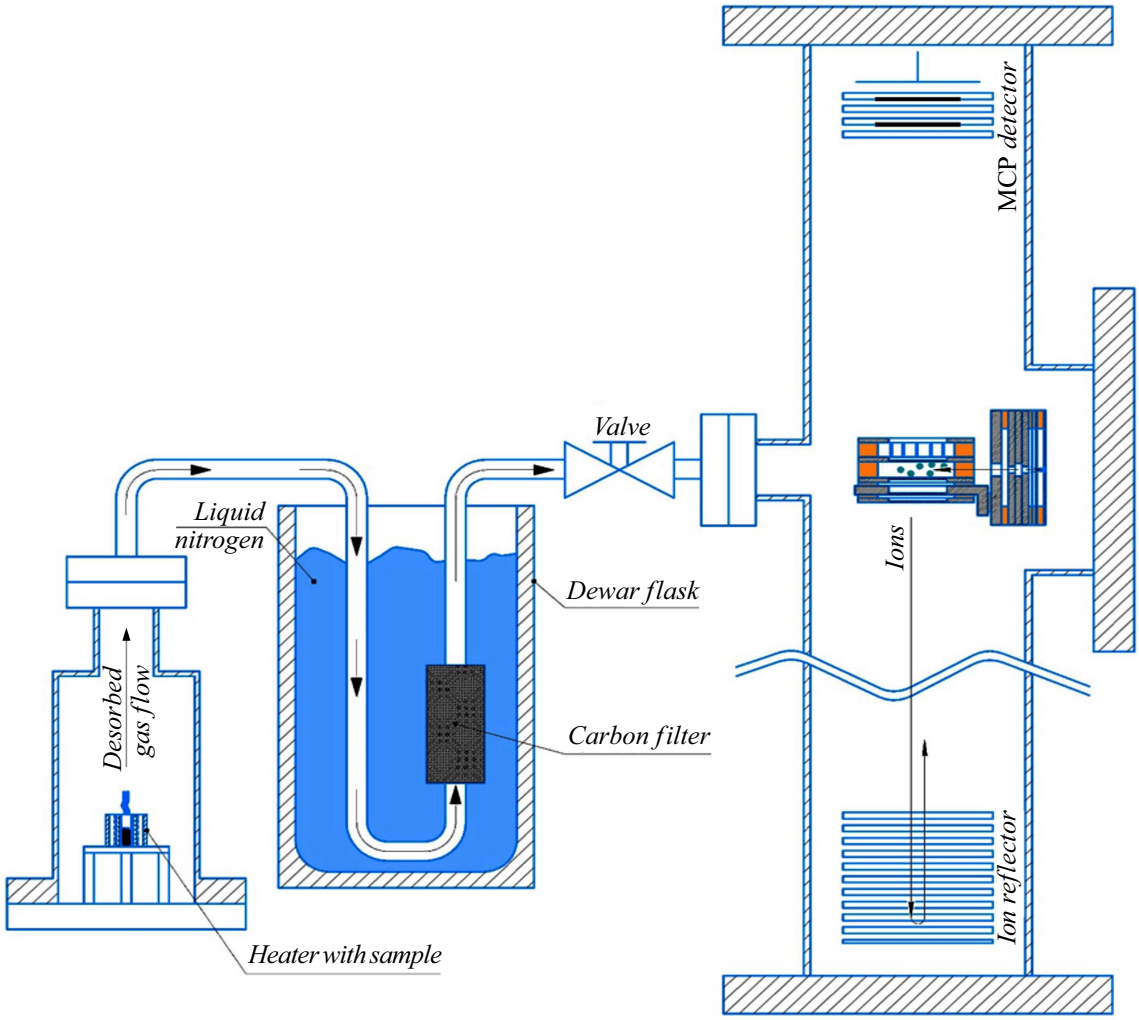

Figure 5. The TOFMS setup using a heater and a cooled carbon filter.

located and for developing a method for cleaning graphite tiles from absorbed gases.

We used another interface in our the study of protective graphite tiles placed in the tokamak (Fig.5), which allowed for the increase of sensitivity and reliable recording of peaks of hydrogen and helium isotopes in these tiles. This interface contains a special reactor, which houses a miniature heater with a quartz crucible for the sample placed in it. The crucible is heated to high temperatures in increments of $\sim 100^{\circ}$C. The gas released from the sample is injected into the ionization region of the mass-reflectron after reaching a certain temperature through a tube having a U-shaped section, the lower part of which is filled with activated carbon and cooled to the temperature of liquid nitrogen.

Such a reactor device is known and is used, for example, in studies of the helium isotopy [22,23]. It allows for almost complete absorption of ordinary chemically active gases released from the sample and increase of the concentration of hydrogen and helium isotopes in the injected gas sample, and thereby increasing the sensitivity of the device to light gases. The admission system with a carbon filter cooled to the temperature of liquid nitrogen operates in the sample accumulation mode, and then the gas is admitted into the ionization zone using an admission valve. Conducted studied [20] showed that this interface allows for about 5-fold increase of the sensitivity of the TOFMS for hydrogen and helium isotopes. Almost the same results were obtained in earlier studies of the content of noble gases in ice cores from a hole drilled in Lake Vostok in Antarctica [24,25]. Several methods of isolation, accumulation and preservation of gas samples were used in these studies, because it was almost a year from the moment the ice core was recovered from a hole with a depth of about 3,500 m to the measurement, for example, $^4He^+/^{20}Ne^+$. Therefore, such unique samples were measured in several laboratories and in different countries. As the content of ^{4}He in atmospheric air is ~ 5.2 ppm, and neon is ~ 18 ppm, we used an interface with activated carbon, cooled to nitrogen temperature for reliable and more accurate registration of these components. However, no significant differences were found in the content of helium and neon isotopes in ice cores in comparison with the usual concentrations of the

respective isotopes in the atmospheric air. However, these measurements of helium and neon isotopes in ice samples and atmospheric air using an interface with activated carbon cooled to nitrogen temperature turned out to be very interesting. The mass spectrum of atmospheric air is shown in Fig. 6. Peaks of molecular hydrogen ($m/z = 2$ amu), atomic nitrogen ($m/z = 14$ amu), water ($m/z = 18$ amu), molecular nitrogen ($m/z = 28$ amu), oxygen (O_2) and argon (Ar) are probably attributable to residual atmospheric air remaining in the interface between the activated carbon and the outlet valve. The peaks of the heavy isotope helium $^4He^+$ ($m/z = 4$ amu), the isotopes neon $^{20}Ne^+$ and $^{22}Ne^+$ are clearly identified in the mass spectrum, and, a twice ionized peak was recorded using TOFMS $^{20}Ne^{2+}$, perhaps, for the first time.

Therefore, the use of this interface allows for conducting a kind of calibration of the sensitivity of the device, using atmospheric air as a reference, which contains known small concentrations of isotopes of neon and helium-4, that we indicated earlier. It is probably possible to estimate the sensitivity of such a technique in tenths of ppm based on the concentration of neon and helium isotopes in the atmosphere.

It was necessary to analyze a liquid, presumably high-quality gasoline or another solvent in one of the completed studies and we used the following technique. The sampler, made of stainless steel and fitted with a heater, was filled with the test liquid. The sampler was connected to the mass spectrometer using a piezoelectric leak valve. The discharge value was controlled automatically at the level of $1 \cdot 10^{-6}$ Torr. The heater allowed for increasing the temperature of the sample to 60°C, and the produced vapor entered the mass spectrometer through the leak valve. It turned out that it was a very poor design for the sampler because the vapor pressure of the heated liquid is very critical for the heating rate, for the amount of the studied liquid, for its properties, for the volume of the sampler. Therefore, we introduced a glass porous membrane into the

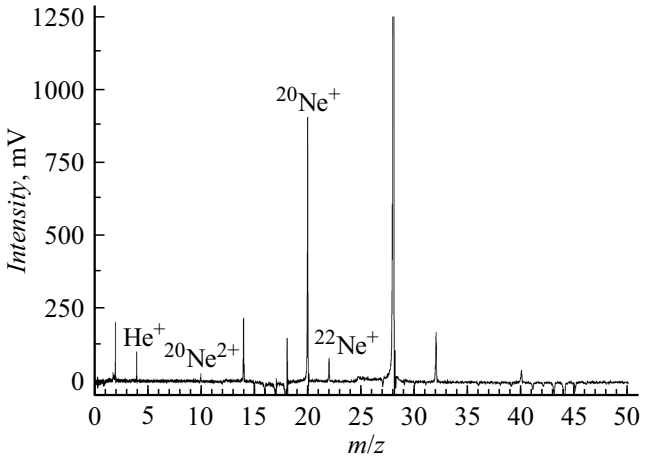

Figure 6. The spectrum of air passed through a carbon filter cooled to the temperature of liquid nitrogen.

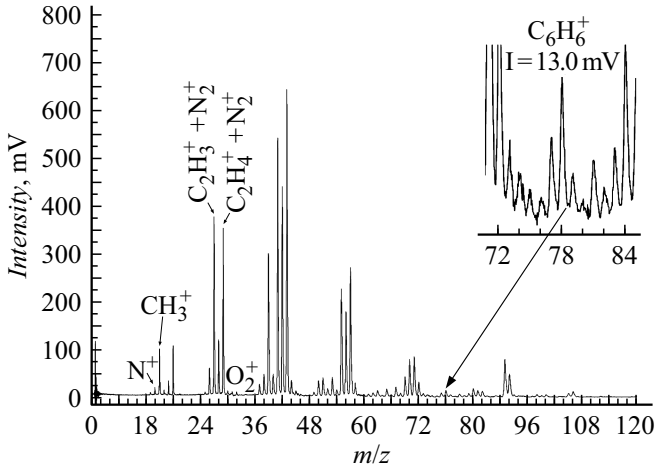

Figure 7. Mass spectrum of AI-95 gasoline vapors at electron energy $U_e = 100$ eV and room temperature $T = 25$°C.

sampler, which separates the volume with the studied liquid sample from the volume used for the admission into the mass spectrometer chamber and a sufficiently low pressure is maintained in the volume with the sample at the level of 10^{-2} Torr using a forevacuum pump. Essentially, this interface can be used to operate a linear TOFMS with both liquid samples and a capillary gas chromatograph [26], since it has all the necessary features for this. The mass spectrum of AI-95 gasoline is shown in Fig. 7. A section of the spectrum in the mass region 72–84 amu is given on an enlarged scale in the upper right part of the figure, which allows for accurate identification of benzene $C_6H_6^+$.

Conclusion

The interfaces developed for the linear TOFMS have significantly expanded the scope of application of the device, made it possible to analyze solid, liquid and gaseous samples, and significantly increased the sensitivity of the device to helium and neon isotopes. We used only an electron shock and a conventional Nier source, in which the electron energy could vary from 10 to 150 eV as an ionization method. A technique for calibration of the sensitivity of mass reflectors using natural standards such as isotopes of helium and neon in atmospheric air is proposed.

Funding

The study was conducted as part of the research program planned at the Ioffe Physical-Technical Institute.

Conflict of interest

The authors declare that they have no conflict of interest.

References

[1] A.E. Cameron, D.F. Eggers. Rev. Sci. Instr., **19**, 605 (1948).
[2] E.I. Agishev, N.I. Ionov. ZhTF, **26** (1), 203 (1956) (in Russian).
[3] E.I. Agishev, N.I. Ionov. ZhTF, **28** (8), 1775 (1958) (in Russian).
[4] N.I. Ionov, B.A. Mamyrin. ZhTF, **23** (11), 2101 (1953) (in Russian).
[5] S.G. Alikhanov. ZhETF **31**, 3 (517 1956) (in Russian).
[6] B.A. Mamyrin. AS. № 198034. BI 13 148 (1967).
[7] V.I. Karataev, B.A. Mamyrin, D.V. Shmikk. ZhTF, **41** (7), 1498 (1971) (in Russian).
[8] B.A. Mamyrin, V.I. Karataev, D.V. Shmikk, V.A. Zagulin. ZhETF **64** (1), 82 (1973) (in Russian).
[9] B.A. Mamyrin, Intern. J. Mass Spectrometry, **206**, 251 (2001).
[10] N.N. Aruyev, V.T. Zhdan, A.V. Kozlovsky, C.N. Markovsky, I.I. Pilyugin, Mass-spektrometriya, **5** (4), 189 (2008) (in Russian).
[11] V.I. Karataev, N.N. Aruev. Pisma v ZhTF, **37** (12), 67 (2011) (in Russian).
[12] V.I. Karataev. Pisma v ZhTF, **24** (5), 1 (1993) (in Russian).
[13] D.V. Afanasyev, G.A. Baranov, A.A. Bogdanov, G. A. Dyuzhev, A.K. Zinchenko, V.I. Karataev, A.A. Kruglikov. Pisma v ZhTF, **25** (18), 12 (1999) (in Russian).
[14] V.I. Karataev. Pisma v ZhTF, **34** (24), 90 (2008) (in Russian).
[15] B.A. Mamyrin, D.V. Shmikk. ZhETF **76** (5), 1500 (1979) (in Russian).
[16] V.M. Tuchkevich. Vestnik AN, **5**, 9 (1985) (in Russian).
[17] N.N. Aruyev, A.A. Bogdanov, M.I. Petrov, A.M. Polyansky, V.A. Polyansky, R.V. Tyukaltsev, I.L. Fedichkin. Pisma v ZhTF, **35** (14), 40 (2009) (in Russian).
[18] N.N. Aruyev, M.A. Kozlovsky, M.F. Kudoyarov, M.Ya. Patrova, P.A. Romanov, R.V. Tyukaltsev, I.L. Fedichkin, S.V. Filippov. Pisma v ZhTF, **45** (16), 30 (2019) (in Russian).
[19] N.N. Aruyev, A.V. Kozlovsky, I.L. Fedichkin, G.L. Saksagansky. Pisma v ZhTF, **23** (20), 83 (1997) (in Russian).
[20] E.B. Yudina, P.A. Romanov, A.S. Chizhikova, N.N. Aruev. Nanotub. Carbon Nanostruct, **30**, 1 (2022). DOI: http://dx.doi.org/10.1080
[21] N.N. Aruyev, A.N. Novokhatsky, P.A. Romanov, N.V. Sakharov, R.V. Tyukaltsev, S.V. Filippov. Mass-spektrometriya, **20** (1), 18 (2023) (in Russian).
[22] N.N. Aruyev, A.N. Novokhatsky, P.A. Romanov, N.V. Sakharov, S.V. Filippov, P.B. Shchegolev. Pisma v ZhTF, **49** (14), 34 (2023) (in Russian).
[23] B.A. Mamyrin, I.N. Tolstikhin. *Izotopy geliya v prirode* (Energoizdat, M., 1981), 222 p. (in Russian).
[24] Yu.O. Chetverikov, N.N. Aruyev, S.A. Bulat, V.F. Yezhov, V.Ya. Lipenkov, V.A. Solovey, R.V. Tyukaltsev, I.L. Fedichkin. ZhTF, **86** (7), 130 (2016) (in Russian).
[25] Yu.O. Chetverikov, N.N. Aruyev, S.A. Bulat K.A. Gruzdov, V.F. Yezhov, F. Jean-Baptiste, I.L. Kamensky, V.Ya. Lipenkov, E.M. Prasolov, V.A. Solovey, R.V. Tyukaltsev, I.L. Fedichkin. ZhTF, **88** (5), 760 (2018) (in Russian).
[26] R.A. Khmelnitsky, E.S. Brodsky. *Mass-spektrometriya zagryaznenij okruzhayushchej sredy* (Khimiya, M., 1990), 182 p. (in Russian).

Translated by A.Akhtyamov